13th ewtec 2019 Proceedings of the 13th European Wave and Tidal Energy Conference 1-6 Sept 2019, Naples, Italy

Morphing blades for passive load control of tidal turbines

Weidong Dai, Gabriele Pisetta, Ignazio M. Viola

Abstract—**A passive load-control system is proposed to reduce the load fluctuations on tidal turbine blades. Load fluctuations may result in fatigue failures, and thus they are one of the main factors that affect the reliability of tidal turbines. In this paper, we analyse the fluid-structure interaction of surface-morphing blades. While the results can be equally applied to wind and tidal turbines, a tidal turbine blade is chosen as a test case. We consider a bi-dimensional model that can represent two possible physical designs: (1) a blade with a flexible trailing edge from root to tip and, (2) a rigid blade that can passively rotate around its pitch axis. We show that both designs are capable of almost perfect cancellation of the load fluctuations without affecting the mean power generated. The optimal structural parameters are identified by a mathematical model based on first principles. The morphing blade is modelled with a mass-damper-spring system which is weakly coupled to a hydrodynamic model. The optimum blade design is then tested with unsteady Reynolds-averaged Navier-Stokes simulations. The CFD results show that 97% of thrust fluctuations can be cancelled for the same amount of energy extracted than rigid blades.**

Keywords—**gust alleviation, load control, morphing blade, passive pitch.**

I. Introduction

A Xial-flow horizontal-axis tidal turbine experience significant fatigue loading due to the inherent unsteadiness of the flow. The shear layer, the high turbulent kinetic energy in the tidal stream [1, 2] and the wave-induced currents [3] represent critical loading conditions in the design of the turbine's blade. The uncertainty associated with these unsteady loads is mitigated by designing blades with high safety factors which leads to over-engineered blades and high capital costs [4]. Therefore, reducing the fluctuations of the loads experienced by the blades will reduce their cost and the levelized cost of energy.

Individual pitch control is the most advanced active control system employed at a commercial scale both for wind and tidal turbines [5, 6]. Individual pitch control would significantly mitigate load fluctuations, however, it is seldomly used in the tidal industry because of the increased complexity and the consequent loss of reliability.

Moreover, with the scale up to larger devices, the turbine diameter becomes closer to the size of the most energetic turbulent eddies in the flow stream [7] and the increase in the blade flexibility leads to higher aeroelastic coupling [8].

Different load-mitigating technologies have been investigated in the aeronautical industry, and trailing-edge flaps, whether with a rigid or a flexible structure are indicated as the most promising device [9-12]. Therefore, we believe that morphing blades could prove very effective to alleviate fatigue loads on the blades of a tidal turbine.

Research about load alleviation systems for tidal turbines is limited, with a few studies about individual pitch control [13] and camber control [14-16]. To our knowledge, Tully and Viola [14] are the only ones who studied how to alleviate loads on tidal turbines using morphing blades. They found that, under current and opposing wave conditions, the passive deflection of a blade section can reduce the loads fluctuations up to 30%.

In this paper, we present a novel passive load control system inspired by this morphing blade concept and we show that it cancels almost completely the loads fluctuations.

A. A simple model of a morphing blade

Morphing blades are regarded as a camber control system. A passive morphing blade works by aligning part of its structure towards the instantaneous flow direction, similar to a wind vane. Fig. 1 shows that when the angle of attack is increased by $\Delta\alpha$ due to unsteady inflow conditions, the fluid loading increases, and the pressure generates a moment that bends the morphing blade upwards. The deformation has a decambering effect on the blade, hence the effective angle of attack is reduced by $\Delta\beta$. The change of the angle of attack is thus $\Delta\alpha - \Delta\beta$, therefore the load increase is mitigated. The load-alleviating

Paper ID number: 1461- Conference track:Tidal device development and testing.
This work was supported in part by the EPSRC, project reference number EP/L016680/1 and in part by the Edinburgh Global Research Scholarship.

W. Dai is a PhD candidate at the School of Engineering, Institute for Energy Systems (IES), the University of Edinburgh, Edinburgh, EH9 3BF, UK (e-mail: w.dai@ed.ac.uk).

G. Pisetta is a PhD candidate at the School of Engineering, Institute for Energy Systems (IES), the University of Edinburgh, Edinburgh, EH9 3BF, UK (e-mail: gabriele.pisetta@ed.ac.uk).

I. M. Viola is Senior Lecturer at the School of Engineering, Institute for Energy Systems (IES), the University of Edinburgh, Edinburgh, EH9 3BF, UK (e-mail: I.M.Viola@ed.ac.uk).

performance of the morphing blade is determined by the flexibility of its material.

We present a simple model of a passive morphing foil where the flexibility of the foil is represented by a torsional spring of stiffness κ (Fig. 1). The foil is considered rigid and the spring controls its angular position around a chosen axis. The change of the foil camber is represented by a change in the actual angle of attack caused by the passive pitching of the blade. As long as the effect of the

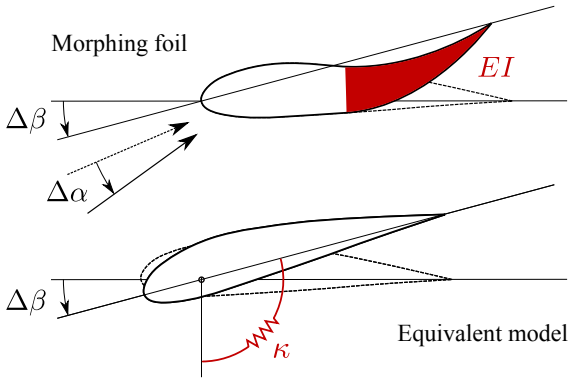

Fig. 1. Morphing foil and the equivalent passive pitch model. The foil compliance is modelled by a torsional spring with stiffness κ.

thickness and the exact shape of the foil on the unsteady lift are negligible, the two models in Fig. 1 are equivalent. This is a reasonable approximation when flow separation does not occur. Hence, the validity of the model breaks down near the root, where dynamic stall might occur.

We analyze the performances of this load control system for a 2D section of a tidal turbine blade subjected to load fluctuations due to the shear flow. We investigate whether it is possible to mitigate the load fluctuations without affecting the mean power generated. Firstly, we identify the optimal structural parameters using an analytical model based on first principles. Then, the optimum blade design is tested using unsteady Reynolds-averaged Navier-Stokes (RANS) simulation.

II. METHODOLOGY

The passive pitch system is described in Fig. 2, where α is the angle of attack, U is the inflow velocity, β is the pitch angle, β_0 is the geometric twist of the blade, $\theta = \theta_0 + \delta\theta$ is the extension of the spring and $\phi = \alpha + \beta$ is the inflow angle. We adopt a linear spring with constant stiffness κ.

The blade rotates about the axis at $x_A = 0.1c$, where c is the chord. Under steady inflow conditions, the foil experiences constant inflow velocity $\overline{U}$ and constant angle of attack $\overline{\alpha}$ that generate a positive hydrostatic moment

$$M_{hs} = \frac{1}{2}\rho_w c^2 \overline{U}^2 C_M(\overline{\alpha}), \tag{1}$$

where ρ_w is the water density and C_M is the moment coefficient, which depends on α.

We define the preload angle θ_0 as the spring deformation required to balance the hydrostatic moment:

$$\theta_0 = \frac{1}{\kappa}\left(\frac{1}{2}\rho_w c^2 \overline{U}^2 C_M(\overline{\alpha})\right), \tag{2}$$

When considering unsteady inflow conditions, the spring deformation is composed by two terms: the preload angle θ_0 balances the moment arising from the average inflow conditions, and $\delta\theta$ counteracts the fluctuations around the mean caused by the unsteadiness of the flow. The next paragraphs will explain how we defined the unsteady inflow conditions for the test case and how we solved the dynamic problem of a passively pitching foil subjected to inflow fluctuations.

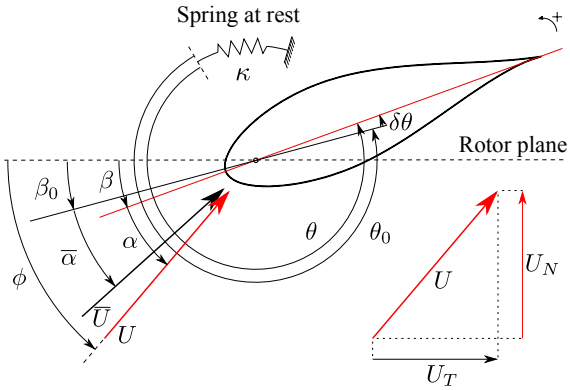

Fig. 2. Passive pitch system. The spring preload angle θ_0 balances the moment arising from the mean flow, whereas the deflection $\delta\theta$ compensates the fluctuations around the mean flow.

B. *Inflow conditions*

We use a code based on blade element momentum theory to compute the inflow conditions for a 3 blades, 1MW axial flow tidal turbine operating at constant speed in a shear flow. The inflow for each section of the blades is determined by two velocity components: the fluid speed U_T relative to the blade rotation that acts tangential to the plane of the rotor, and the speed U_N of the tidal current that travels perpendicular to the rotor plane. The shearing is due to the boundary layer of the seabed. The velocity profile is such that during its rotation the blade experiences a varying velocity U_N (Fig. 2).

As a consequence, the inflow velocity for each section changes periodically both in its magnitude $U = \sqrt{U_T^2 + U_N^2}$ and its direction $\phi = \text{atan}\left(\frac{U_N}{U_T}\right)$. We define the average flow conditions as

$$\begin{aligned} \overline{U} &= \sqrt{U_T^2 + \overline{U}_N^2}, \\ \overline{\phi} &= \text{atan}\left(\frac{\overline{U}_N}{U_T}\right), \end{aligned} \tag{3}$$

where $\overline{U}_N$ is the average speed of the tidal flow experienced by a blade section over one revolution and it is defined as

$$\overline{U}_N = \frac{1}{2\pi}\int_0^{2\pi} U_N \, d\psi, \tag{4}$$

where ψ indicates the angular position of the turbine blade during its revolution.

For a rigidly fixed blade, the average angle of attack is computed for each section as

$$\overline{\alpha} = \overline{\phi} - \beta_0, \tag{5}$$

where β_0 is the geometric twist of the section.

To compute the unsteady loading resulting from the periodic onset flow velocity fluctuations, we used Theodorsen's theory [17]. With this approach, the small effect of the foil thickness is neglected. Interested readers could consider improving the current model by accounting for the effect of the camber following Motta et al. [18] The inflow fluctuations are approximated with a sinusoidal shape as shown in Fig. 3. We determined the oscillations of U_N such that the angle of attack α would

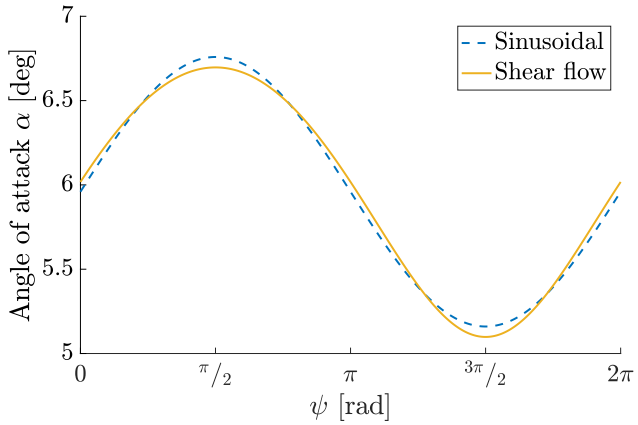

Fig. 3. Angle of attack fluctuations. The oscillations generated by the shear flow are approximated using a sinusoidal shape with the same mean value and the same amplitude.

fluctuate harmonically, with the same amplitude and the same mean value as for the inflow conditions due to the shear flow.

TABLE I
BLADE PROPERTIES AND FLOW CONDITIONS

Mean angle of attack [deg]	$\overline{\alpha}$	5.96
Angle of attack fluctuations [deg]	$\Delta\alpha$	±0.80
Twist angle [deg]	β_0	5.39
Chord [m]	c	1.02
Mean inflow speed [ms^{-1}]	$\overline{U}$	6.98
Reynolds number [-]	Re	7.11×10^6
Inflow speed fluctuations [ms^{-1}]	ΔU	±0.019
Pitch axis position [-]	x_A/c	0.10
Sea water density [kgm^3]	ρ_w	1025
Sea water viscosity [m^{2}s^{-1}]	ν	1.05×10^{-6}
Foil inertia [kgm]	J	278
Fluctuations frequency [rads^{-1}]	ω	1
Fluctuations reduced frequency [-]	$k = \frac{\omega c}{2\overline{U}}$	0.073
Foil type		NACA $63_{(318)}$427

We consider the blade section at 75% of blade span. The blade section properties and the local flow conditions are summarized in Table I.

C. *Quasi-steady model*

Since the unsteadiness of the flow is relatively low ($k \ll 1$), firstly we analyse the problem using a quasi-steady approach. The spring moment reaction is

$$M_\kappa = -\kappa\theta, \tag{6}$$

and the hydrostatic moment is

$$M_{hs} = \frac{1}{2}\rho_w c^2 U^2 C_M(\alpha), \tag{7}$$

Since the system is designed to operate around the average flow conditions, the moment coefficient is linearized as

$$C_M(\alpha) = C_{M,\alpha}\alpha + C_{M,0} \tag{8}$$

where the terms $C_{M,\alpha}$ and $C_{M,0}$ are obtained from a linear regression performed over the range $\overline{\alpha} \pm 3$ deg. For each incidence value, the flow field is simulated using unsteady RANS simulation. Once the simulation has reached a steady state, we extract the values of C_M to inform the linear regression.

The equilibrium position of the blade is determined at each time step by balancing the spring reaction and the hydrostatic moment, such that

$$M_\kappa + M_{hs} = 0. \tag{9}$$

By noting that $\beta = \beta_0 + \delta\theta$, where $\delta\theta = \theta - \theta_0$, and recalling that $\phi = \alpha + \beta$ and $\alpha = \overline{\alpha} + \delta\alpha$, we obtain

$$\alpha = \phi - \beta_0 - \theta + \theta_0. \tag{10}$$

Using (10), (9) is solved and the equilibrium position of the blade is evaluated as

$$\theta = \frac{1}{\kappa}\left(\frac{\frac{1}{2}\rho_w c^2 U^2\left[C_{M,\alpha}(\phi - \beta_0 + \theta_0) + C_{M,0}\right]}{\kappa + \frac{1}{2}\rho_w c^2 U^2 C_{M,\alpha}}\right) \tag{11}$$

The angle of attack is readily evaluated using (10) and the lift L and the drag D on the blade section are computed as

$$\begin{aligned} L &= \frac{1}{2}\rho_w U^2 c C_L(\alpha), \\ D &= \frac{1}{2}\rho_w U^2 c C_D(\alpha) \end{aligned} \tag{12}$$

where C_L and C_D are the static lift and drag coefficient and are informed by unsteady RANS simulations. We express the loads with reference to the plane of the turbine rotor as

$$\begin{aligned} N &= L\cos\phi + D\sin\phi\,, \\ T &= L\sin\phi - D\cos\phi\,, \end{aligned} \tag{13}$$

where N acts in the direction of U_N, and T acts in the opposite direction of U_T (Fig. 2). The load coefficients are respectively defined as

$$\begin{aligned} C_N &= \frac{N}{\frac{1}{2}\rho_w \overline{U}^2 c}, \\ C_T &= \frac{T}{\frac{1}{2}\rho_w \overline{U}^2 c}. \end{aligned} \tag{14}$$

D. Dynamic model

We also quantify the dynamic effects using Theodorsen's unsteady linear theory [17].

The position of the blade is determined by balancing the moments with respect to the pitch axis, where the reaction of the spring is defined as for the quasi-steady case using (6). Instead, the hydrodynamic moment is based on Theodorsen's equation for the harmonic pitching of a rigid foil. The original formulation of Theodorsen for the unsteady loads on a foil was developed for a flat plate at zero incidence. Hence, the equations are cast for the fluctuations of the angle of attack around its mean value $\delta\alpha = \alpha - \overline{\alpha}$, but they also account for the loads due to the average angle of attack.

The resulting moment is a function of the angle of attack fluctuations $\delta\alpha$, the pitch rate $\delta\dot{\theta}$, and the respective time derivatives $\delta\dot{\alpha}, \delta\ddot{\theta}$. The hydrodynamic moment is thus computed as

$$M_{hd} = X\delta\ddot{\theta} + Y\delta\dot{\theta} + W\delta\dot{\alpha} + Z\delta\alpha + M_{hs}, \tag{15}$$

where

$$\begin{aligned} X &= \rho_w b^4 \pi \left(\frac{1}{8} + \left(\frac{d}{b}\right)^2\right), \\ Y &= -\rho_w U b^3 \pi \left(\frac{1}{2} + \frac{d}{b}\right) C(k) \left(1 - 2\frac{d}{b}\right), \\ W &= \rho_w b^3 \pi \left(\frac{1}{2} - \frac{d}{b}\right) U, \\ Z &= \frac{1}{2}\rho_w U^2 c^2 C_{M,\alpha} C(k). \end{aligned} \tag{16}$$

In the above equations, $C(k)$ is Theodorsen's circulation function for a given reduced frequency k, b is the semichord and $d = x_A - b$, in accordance with the original notation used by Theodorsen [17].

We model the pitching blade with a mass-damper-spring system, such that the dynamics of the blade rotation are described by

$$M_{hd} + M_\kappa - \mu\dot{\theta} = J\ddot{\theta}, \tag{17}$$

where μ represents the material damping of the foil, and J is the section inertia to rotation around its pitch axis.

Recalling $\alpha = \overline{\alpha} + \delta\alpha$, (10) is conveniently written as

$$\delta\alpha = \delta\phi - \delta\theta, \tag{18}$$

where $\delta\phi = \phi - \overline{\alpha} - \beta_0$. Equation (18) highlights the dependency of the angle of attack oscillations on the fluctuations of the inflow $\delta\phi$ and the blade pitch $\delta\theta$. Moreover, using (18) it is possible to express the hydrodynamic moment as a function of $\delta\theta$ and $\delta\phi$, hence the dynamic equation can be cast as

$$\begin{aligned} (J - X)\delta\ddot{\theta} + (W - Y + \mu)\delta\dot{\theta} + (Z + \kappa)\delta\theta \\ = W\delta\dot{\phi} + Z\delta\phi, \end{aligned} \tag{19}$$

where the only unknown are $\delta\theta$ and its derivatives.

The dynamic equation is solved by transforming (19) to the frequency domain. The fluctuations induced by the shear flow are periodic, such that $\delta\phi = \frac{\Delta\phi}{2}\exp(j\omega t)$, where $\Delta\phi$ is the amplitude of the fluctuations, ω is the frequency of the fluctuations and j is the imaginary unit. Hence, we expect the blade to oscillate with $\delta\theta = \frac{\Delta\theta}{2}\exp\big(j(\omega t + \eta)\big)$. By substituting $\delta\dot{\theta} = j\omega\delta\theta$, $\delta\ddot{\theta} = -\omega^2\delta\theta$, $\delta\dot{\phi} = j\omega\delta\phi$ and $\delta\dot{\phi} = -\omega^2\delta\phi$, (19) is rewritten as

$$\begin{aligned} [-\omega^2(J - X) + j\omega(W - Y + \mu) + Z + \kappa]\delta\theta \\ = (j\omega W + Z)\delta\phi. \end{aligned} \tag{20}$$

The dynamics of $\delta\theta$ are determined by the algebraic solution of the above complex equation for each time step. We compute the evolution of the angle of attack using (18), hence the loads acting on the foil are evaluated. The lift is determined according to Thedorsen's theory as

$$\begin{aligned} L = \pi\rho_w b^2 &\left[U\delta\dot{\alpha} - b\left(\frac{d}{b}\right)\delta\ddot{\theta}\right] \\ &+ 2\pi\rho_w U b^2 C(k)\left(\frac{1}{2} - \frac{d}{b}\right)\delta\dot{\theta} \\ &+ \frac{1}{2}\rho_w U^2 c\big[C(k)C_{Ls}(\alpha) + \big(1 - C(k)\big)C_{Ls}(\overline{\alpha})\big]. \end{aligned} \tag{21}$$

Being based on the assumption of potential flow, Theodorsen's theory predicts zero drag, hence the drag is computed as for the quasi-steady case using (12). The normal and tangential forces for the dynamic case are evaluated using (13), and the respective coefficients are computed using (14).

The analysis is generalized by introducing the non-dimensional coefficients for the stiffness Γ and the damping C_μ, respectively defined as

$$\begin{aligned} \Gamma &= \frac{\kappa}{\frac{1}{2}\rho_w c^2 \overline{U}^2}, \\ C_\mu &= \frac{\mu}{\frac{1}{2}\rho_w c^2 \overline{U}^2 \omega^{-1}}. \end{aligned} \tag{22}$$

E. *Control system optimization*

The optimization problem consists in finding the system design that minimizes the flapwise bending moment fluctuations on the blade over its revolution, with the requirement that the mean power extracted from the flow is the same as for the turbine with rigidly attached blades. For the bi-dimensional test case, we seek the spring properties that minimize the fluctuations of the normal force ΔC_N whilst keeping constant the average value of the tangential force $\overline{C}_T$. The 2D optimization problem is thus defined as

$$\begin{aligned} &\min_{\kappa} \hat{f}(\kappa) = \Delta C_N \\ &\text{s.t.} \quad \frac{\partial \overline{C}_T}{\partial \kappa} = 0. \end{aligned} \tag{23}$$

We solve the problem using an exhaustive search algorithm. Hence, we test a wide range of spring and we select the one that minimizes the load fluctuations. The requirement of constant $\overline{C}_T$ is satisfied by assuring a constant pitch angle $\beta = \beta_0$ for average inflow conditions $\overline{\alpha}$ and $\overline{U}$. This method approximates the average loads with the loads generated by average flow conditions, namely $\overline{C}_T \cong C_T(\overline{\alpha}, \overline{U})$. Using this approximation, we obtain that the preload angle θ_0 ensures the compliance with the optimization constraint, as shown in (2).

The optimization problem stated in (14) is applied to the quasi-steady model as well as to dynamic model. The optimal spring parameters determined with the dynamic model are thus validated via unsteady RANS simulations.

F. *CFD analysis*

The computational fluid dynamics calculations are performed in STAR-CCM+. An unstructured mesh of ca. 10^6 cells, was constructed with ICEM, and used to discretize the computational domain $\Omega = \left\{\frac{x}{c} \in [-20, 50] \times \frac{y}{c} \in [-20, 20]\right\}$. Radial basis functions are used to morph the mesh at every time step. We use a $k-\omega$ SST two-equations turbulence model, and a second order implicit finite difference Newmark-Wilson scheme is applied to approximate the blade angular velocity and its position at time-step N as

$$\begin{aligned} \dot{\theta}_N &= \dot{\theta}_{N-1} + \left[\gamma \ddot{\theta}_N + (1-\gamma)\ddot{\theta}_{N-1}\right]\Delta t, \\ \theta_N &= \theta_{N-1} + \dot{\theta}_{N-1}\Delta t + \left[\epsilon \ddot{\theta}_N + \left(\frac{1}{2} - \epsilon\right)\ddot{\theta}_{N-1}\right]\Delta t^2, \end{aligned} \tag{24}$$

where Δt is the time-step, $\gamma = 1/2$ and $\epsilon = 1/4$. To calculate the angular acceleration of the blade, the classic mass-spring system with one degree of freedom is used

$$J\ddot{\theta} + \kappa\theta = M, \tag{25}$$

where M is the resultant moment acting on the body with respect to the specified axis of rotation.

III. RESULTS

We present here the results for the passive pitch control applied to a 2D foil. The analysis is conducted on the blade section at 75% of the blade span of a 3 blades, 1MW axial-flow tidal turbine, rotating at constant speed in a shear flow. For a rigidly fixed blade, Fig. 4 shows the flow field on the blade section at two different positions. The flow field is very similar between the two blade positions. However, the angle of attack varies by more than 1.5 deg,

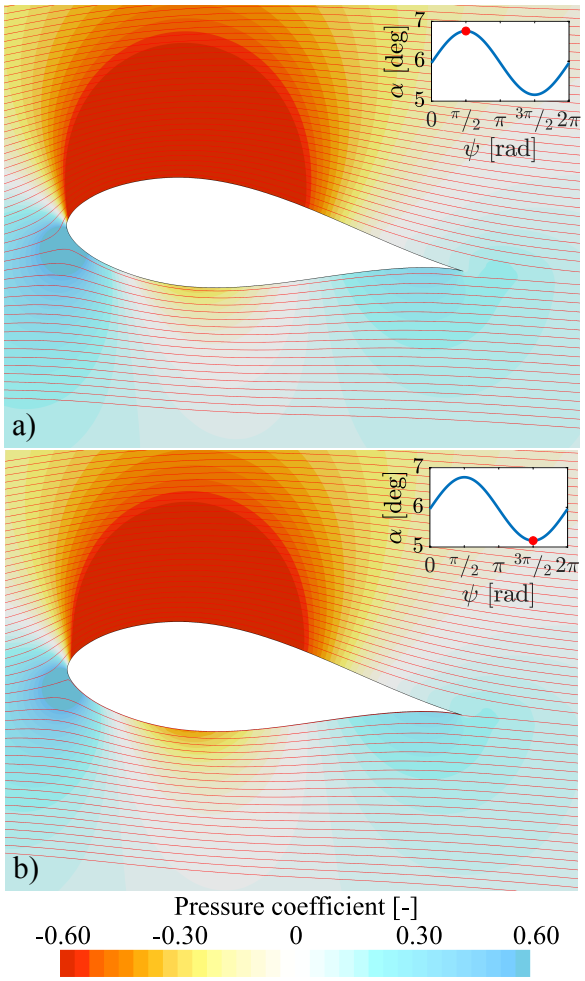

Fig. 4. Pressure contours and streamlines close to the rigidly fixed foil. The foil is subjected to inflow fluctuations and it is depicted at the instants when the angle of attack reaches its maximum (a) and when it reaches its minimum (b), as shown by the insets.

which generates fluctuations of the normal force coefficient with amplitude greater than 15% of its average value.

Figs. 5 and 6 show the CFD loads obtained for the optimized morphing foil and the rigid foil. We chose the spring parameters such that a 10% change of the spring stiffness would cause a negligible improvement of the system performance. Using a spring with stiffness $\Gamma = 10^{-3}$ and preload $\theta_0 = 222$ deg, the fluctuations of C_N are almost completely cancelled. Nonetheless, the mean tangential force, and thus the power extracted, is not affected by the passive pitch system, whereas the amplitude of the fluctuations of C_T are slightly reduced for the morphing foil.

TABLE II
LOAD REDUCTION FOR THE OPTIMIZED CONTROL SYSTEM

	Normal force fluctuations ΔC_N	
	% average C_N	% reduction
Rigid foil	15.59	–
Morphing foil	0.49	97

The results outlined in the table refer to a passive pitch system that employs a torsional spring with $\Gamma = 10^{-3}$ and a preload angle $\theta_0 = 222$ deg.

Table II summarises the comparison between the rigid and the morphing foil configuration. We recall that the normal and the tangential force coefficients are locally representing the thrust and power coefficients of the turbine respectively. Therefore, the passive pitch system alleviates the fatigue loads associated with the blade root flapwise bending moment without compromising the power generation of the device.

Fig. 7 shows a comparison of the loads computed with CFD and the low-order model. The graph shows the difference between the normal force for the rigid foil $C_N|_{\kappa\to\infty}$ and that for morphing foil C_N. For both methods the same spring properties have been used and the blade damping μ was neglected. The two methods predict a similar reduction in the loads.

Given the agreement between the two models, we use the low-order model to conduct a parametric study of the effects of the blade stiffness Γ and the material damping C_μ. Fig. 8 shows the amplitude of the normal force coefficient ΔC_N for a range of stiffness and damping values. Each line presents constant C_μ and it is plotted for the whole range of Γ considered.

For a very stiff torsional spring (high Γ), the load amplitude tends to that of the rigid foil. Instead, by decreasing the spring stiffness, the load amplitude tends asymptotically to different values depending on the damping. A foil that presents high damping values reduce the load-mitigating capability of the system substantially. Moreover, the optimal working condition (i.e. the minimum load amplitude ratio) is achieved with stiffer springs. The quasi-steady model predicts an optimal design point where the loads fluctuations are completely cancelled. This shows that unsteady effects are undesirable, although generally small.

With analogy to a mass-spring-damper system, we define the damping ratio as

$$\xi = \frac{\mu}{2\sqrt{J\kappa}}. \tag{26}$$

The damping ratio is $\xi \ll 1$ for $C_\mu \leq 10^{-1}$. Hence, the two curves for $C_\mu = 10^{-1}$ and 10^{-2} overlap. For $C_\mu > 10$, the damping ratio is $\xi > 1$ over almost the entire range of Γ, however, the system is highly overdamped ($\xi \gg 1$) for low stiffness values and its response greatly differs from that of an undamped system. For high spring stiffnesses, the damping ratio becomes small for any value of C_μ, the stiffness dominates the dynamics of the system and all the curves converge. For the intermediate value $C_\mu = 1$, the system is underdamped ($\xi < 1$) for high stiffness values and becomes overdamped ($\xi > 1$) for $\Gamma < 10^{-4}$.

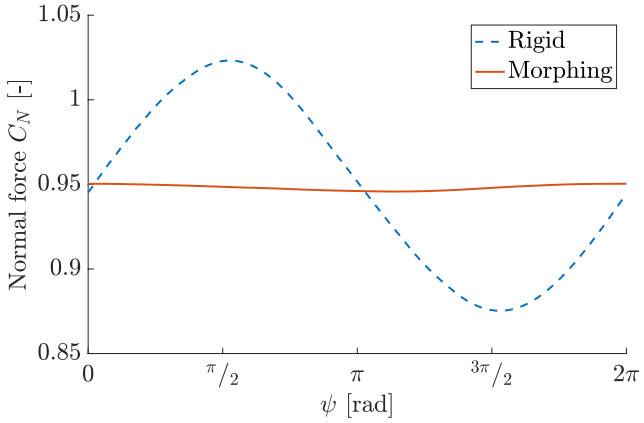

Fig. 5. Normal force coefficient. The dashed line is used for the rigid blade, the continuous line is used for the morphing blade modelled as a passively pitching blade.

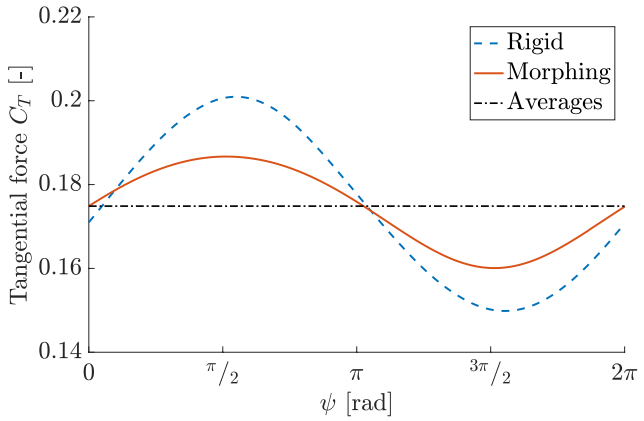

Fig. 6. Tangential force coefficient. The dashed line is used for the rigid blade, the continuous line is used for the morphing blade modelled as a passively pitching blade.

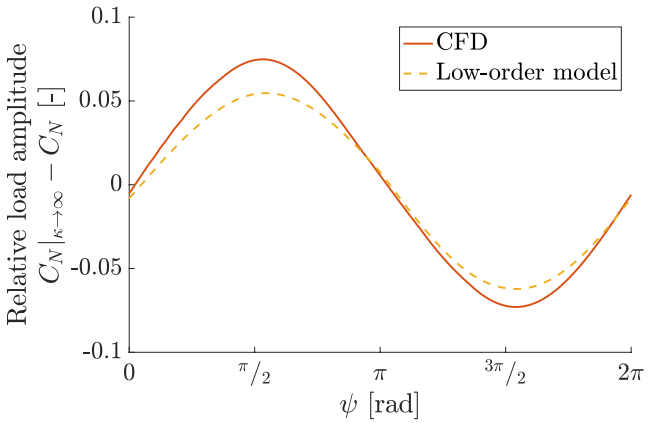

Fig. 7. Comparison between CFD and low-order model results. The y-axis shows the difference between the normal force coefficient on the rigid blade $C_N|_{\kappa\to\infty}$ and that on the morphing blade C_N.

Theodorsen described the unsteady hydrodynamics by superimposing the effects of the added mass, the pitch rate and the quasi-steady loads corrected for the wake presence. These terms affect the dynamic of the system with effects analogous to additional mass, damping and stiffness respectively, as shown in (19). The damping ratio is computed again to account for these additional effects.

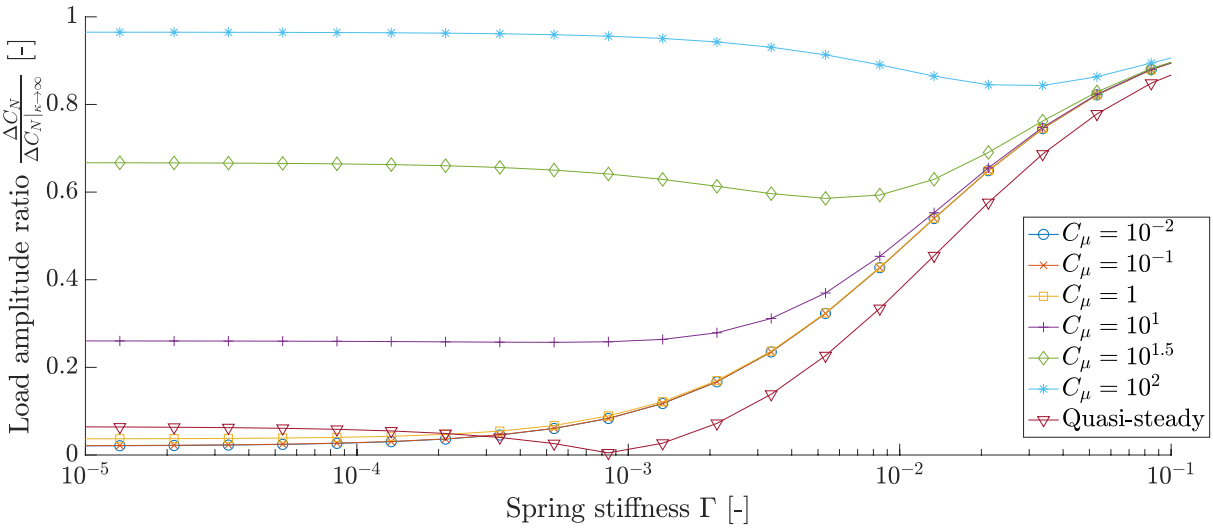

Fig. 8. Passive pitch system performance for different values of the spring stiffness Γ and the material damping C_μ. The y-axis expresses the amplitude of the C_N fluctuations as a fraction of the fluctuations on the rigid foil. It takes the value of 1 for ineffective control and 0 for perfect load cancellation.

The hydrodynamic loads do not change the behaviour of the system. Hence, its dynamics are determined by the foil inertia J, the material damping μ and the stiffness Γ.

IV. Conclusions

The unsteadiness of the flow in tidal channels is responsible for premature fatigue failures of tidal turbines blades. This paper investigated the potential of morphing blades to passively adapt to the changes of the flow in order to alleviate the amplitude of the load fluctuations. In particular, we presented a novel design where a morphing blade is modelled as a passively pitching system. Such model describes the blade compliance using a torsional spring that controls the deflection of a rigid foil.

Using a low-order code based on classic unsteady aerodynamic theory, we designed an optimal control system that is capable of almost complete cancellation of the amplitude of the oscillations of the bending moment coefficient whilst keeping constant the mean power generated by the turbine.

The CFD analysis of the system performances revealed that by using a spring with optimal stiffness and preload it is possible to almost completely cancel the fluctuations of the flapwise force on the blade, with no reduction in the mean power extracted.

The low-order model was then used to investigate the effect of material stiffness and damping on the performances of the morphing blade. For low stiffness values, the system performance is highly affected by the damping, and high material damping decreases the effectiveness of the system.

References

[1] Chamorro, L. P., et al. "On the interaction between a turbulent open channel flow and an axial-flow turbine." *Journal of Fluid Mechanics* 716 (2013): 658-670.

[2] Scarlett, G. and Viola, I. M. "Unsteady Tidal Turbine Blade Loading; an Analytical Approach." *In: 5th Oxford Tidal Energy Workshop 6*. pp. 26-27, 2016

[3] Barltrop, N., et al. "Wave-current interactions in marine current turbines." Proceedings of the Institution of Mechanical Engineers, Part M: *Journal of Engineering for the Maritime Environment* 220.4 (2006): 195-203.

[4] Gaurier, Benoît, et al. "Flume tank characterization of marine current turbine blade behaviour under current and wave loading." *Renewable Energy* 59 (2013): 1-12.

[5] Larsen, Torben Juul, Helge A. Madsen, and Kenneth Thomsen. "Active load reduction using individual pitch, based on local blade flow measurements." *Wind Energy: An International Journal for Progress and Applications in Wind Power Conversion Technology* 8.1 (2005): 67-80.

[6] Shen, Xin, Xiaocheng Zhu, and Zhaohui Du. "Wind turbine aerodynamics and loads control in wind shear flow." *Energy*36.3 (2011): 1424-1434.

[7] Bossanyi, Ervin A. "Individual blade pitch control for load reduction." *Wind Energy: An International Journal for Progress and Applications in Wind Power Conversion Technology* 6.2 (2003): 119-128.

[8] Ng, Bing Feng, et al. "Aeroservoelastic state-space vortex lattice modeling and load alleviation of wind turbine blades." *Wind Energy* 18.7 (2015): 1317-1331.

[9] Barlas, Thanasis K., and Gijs AM van Kuik. "Review of state of the art in smart rotor control research for wind turbines." *Progress in Aerospace Sciences* 46.1 (2010): 1-27.

[10] Lachenal, Xavier, Stephen Daynes, and Paul M. Weaver. "Review of morphing concepts and materials for wind turbine blade applications." *Wind energy* 16.2 (2013): 283-307.

[11] Bottasso, Carlo L., et al. "Load mitigation for wind turbines by a passive aeroelastic device." *Journal of Wind Engineering and Industrial Aerodynamics* 148 (2016): 57-69.

[12] Cordes, Ulrike, et al. "Experimental investigation of Passive Load Reduction under dynamic inflow conditions." *33rd AIAA Applied Aerodynamics Conference*. 2015.

[13] Hu, J., Willden, R. H. J., "Unsteady load relief of an axial flow tidal turbine in sheared flow by individual pitch control." *In: 5th Oxford Tidal Energy Workshop*. 50-51, 2016

[14] Young, A., Farman, J., "Adjustable camber for extended fatigue life." *In: 5th Oxford Tidal Energy Workshop.* pp. 32-33, 2016

[15] Young, A. M., J. R. Farman, and R. J. Miller. "Load alleviation technology for extending life in tidal turbines." *Progress in Renewable Energies Offshore-Proceedings of 2nd International Conference on Renewable Energies Offshore*. 2016.

[16] Tully, S. and Viola, I. M. "Reducing the wave induced loading of tidal turbine blades through the use of a flexible blade." *16th International Symposium on Transport Phenomena and Dynamics of Rotating Machinery*. 2016.

[17] Theodorsen, T. "General theory of aerodynamic instability and the mechanism of flutter". NACA Report (1935).

[18] Motta, V., Guardone, A. and Quaranta, G. "Influence of airfoil thickness on unsteady aerodynamic loads on pitching airfoils." *J. Fluid Mech.* 774 (2015): 460–487.